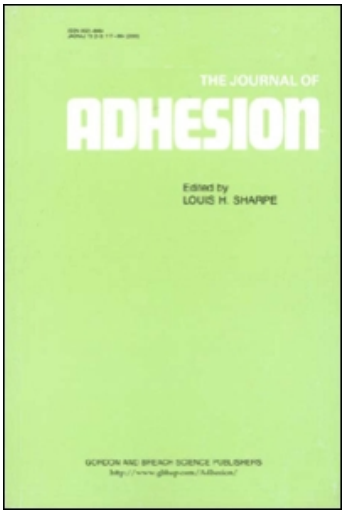

The Journal of Adhesion

Publication details, including instructions for authors and subscription information:
http://www.informaworld.com/smpp/title~content=t713453635

Diffusion of Moisture in Adhesively Bonded Joints

M. M. Abdel Wahab[a]; I. A. Ashcroft[b]; A. D. Crocombe[a]; S. J. Shaw[c]
[a] School of Engineering, University of Surrey, Guildford, UK [b] Wolfson School of Mechanical and Manufacturing Engineering, Loughborough University, Leicestershire, UK [c] Structural Materials Centre, Farnborough, UK

To cite this Article Wahab, M. M. Abdel , Ashcroft, I. A. , Crocombe, A. D. and Shaw, S. J.(2001) 'Diffusion of Moisture in Adhesively Bonded Joints', The Journal of Adhesion, 77: 1, 43 — 80
To link to this Article: DOI: 10.1080/00218460108030731
URL: http://dx.doi.org/10.1080/00218460108030731

The Journal of Adhesion, 77:43–80, 2001

0021-8464/01 $12.00 + .00

Diffusion of Moisture in Adhesively Bonded Joints

M. M. ABDEL WAHAB [a], I. A. ASHCROFT [b], A. D. CROCOMBE [a], and S. J. SHAW [c]

[a]*School of Engineering, University of Surrey, Guildford, UK;*
[b]*Wolfson School of Mechanical and Manufacturing Engineering, Loughborough University, Leicestershire, UK;*
[c]*Structural Materials Centre, Qimetig, Farnborough, UK*

(Received 17 November 2000; in final form 24 May 2001)

In this article, diffusion of moisture in adhesively bonded composite joints is discussed and analysed experimentally, analytically and numerically. The experimental studies concentrate on moisture diffusion in adhesive films and in unidirectional and multi-directional composite substrates exposed to two different conditioning environments, namely 45°C/85% RH and 90°C/97% RH for the absorption studies and 90°C/ambient for the desorption studies. The coefficients of diffusion are determined from the water uptake plots. The analytical solutions for diffusion in joints with impermeable adherends are based on the classical theory of diffusion and are used to derive equations in two-dimensions for different adhesive fillet shapes, namely radiused fillet, triangular fillet and rectangular fillet. In the finite element analysis, the diffusion of moisture from the composite substrates into lap-strap joints is also taken into account. Both unidirectional and multidirectional composites are considered, as well as two different fillet shapes, *i.e.*, rectangular and triangular fillet. A comparison between the results obtained using FEA and those obtained using the analytical solution is made. Finally, fatigue test data for lap-strap joints aged and tested in different environments is presented and a tentative link between fatigue threshold and water concentration at the site of failure initiation is made, indicating a semi-empirical method of predicting the strength of joints subjected to moisture-induced degradation.

Keywords: Diffusion analysis; Composite joints; Durability; FEA; Adhesive bonding; Fatigue

Address correspondence to M. M. Abdel Wahab, School of Engineering (H5), University of Surrey, Guildford, GU2 7XH, UK. E-mail: m.wahab@surrey.ac.uk

INTRODUCTION

Adhesive bonding is used extensively in civil and military aircraft structures and is replacing the traditional joining techniques such as welding, riveting and mechanical fastening. One of the most important advantages of adhesive bonding is its resistance to fatigue, which can lead to a significant reduction in the life-cycle maintenance costs. Another advantage is the substantial reduction in weight, which is of paramount importance for lightweight (*e.g.*, aerospace) structures. In the construction of advanced lightweight composites structures and components, adhesive bonding is usually the most appropriate joining technique in terms of performance and cost. However, mechanical fastening is still the most commonly used joining technique for these materials, primarily because of concerns regarding design, manufacture, certification and non-destructive evaluation of bonded joints and the ability of bonded joints to withstand the aggressive service environments encountered in aerospace applications.

The effect of hostile environmental conditions on the fatigue strength of adhesively bonded structures is, therefore, an important research topic. Moisture can significantly affect the strength of bonded joints and, consequently, a major obstacle to the increased use of adhesive bonding in structural applications is the concern over long-term durability when the joints are exposed to a humid environment. The effect of a hostile environment on joint strength has been demonstrated extensively in the literature, *e.g.* [1]. For metal/epoxy joints, the strength in a hot-wet environment can dramatically be decreased as a function of exposed time, whilst excellent durability is generally observed under dry conditions.

When a metallic joint is exposed to wet environment, water enters the interface either by diffusion through the adhesive layer or by wicking along the adhesive/adherend interface. Many researchers [2–4] have proposed that water mainly enters to the joint through diffusion and that wicking only takes place in the presence of pre-existing micro-cracks or debonded areas at the interface. In the case of polymer composite joints, water diffusion through the composite substrate needs to be taken into consideration. Crank and Park [5] reported that the rate of water diffusion in a polymer can be "non-Fickian", with the diffusion coefficient being dependent on the moisture concentration

and specimen thickness. Lefebvre *et al.* [6–8] presented a comprehensive study of the kinetics of water diffusion in adhesively bonded joints, in which a relation between the diffusion coefficient, temperature, strain and moisture concentration was derived. However, in order to estimate the rate of diffusion in adhesive joints, many authors use the Fickian diffusion model [1, 9, 10].

The loss in joint strength due to water uptake in bonded metal joints is often found to be caused by the degradation of the adhesive/adherend interface rather than weakening of the bulk adhesive [11, 12]. The joint fails cohesively under dry conditions, whilst the interface fails in wet environments [3, 13]. The durability of adhesive joints exposed to a wet environment can be improved by reducing the permeability of the adhesive layer using inert mineral filler, for instance [14], or by improving the durability of the interface using a primer solution [15]. Crocombe [16, 17] presented a numerical technique coupling diffusion and mechanical analysis in order to predict the residual strength of adhesive joints exposed to moisture degradation. He concluded that the wet and dry joint strength could be predicted using the adhesive failure strains.

The use of fibre reinforced polymer composites (FRP's) has increased recently in the construction of aerospace structures in general and in civil and military aircraft in particular. As indicated earlier, a limiting factor in the increased use of adhesive bonding in the aircraft industry is the perceived poor durability when bonded joints are exposed to hostile environmental conditions. Therefore, considerable research efforts have been devoted to the study and improvement of the durability of adhesively bonded structures and, in many cases, properly designed bonded joints have demonstrated excellent durability in humid environments over many years. Unlike the case of adhesively bonded metallic joints, water diffuses through the composite substrates into the adhesive layer in FRP joints. Moreover, the mechanical properties of the composite may be affected by moisture. However, in the case of thermosetting polymeric substrates (such as epoxy based matrix compounds), the adhesive/substrate interface is more stable in the presence of moisture than in the case of metallic substrates and, therefore, interfacial degradation is less likely to occur in the former.

Previous durability work on FRP composite joints at DERA (Defence, Evaluation and Research Agency) concentrated on the

fatigue behaviour of lap-strap and double lap bonded composite joints. The lap-strap joints are representative of the long overlap joints and bonded stiffeners found in typical aerospace structures [18]. The results from tests on the lap-strap joints demonstrated little effect on the fatigue threshold when the samples were aged in a humid environment until saturation and then tested at ambient temperature [19]. However, a combination of a high level of moisture (*i.e.*, ageing wet) and testing at elevated temperatures had a significant deleterious effect on the fatigue threshold. This was attributed to the reduction in the glass transition temperature (T_g) of the adhesive as water is absorbed. When T_g approaches the test temperature, a sharp reduction in the mechanical properties of the adhesive occurs, which drastically reduces the fatigue resistance of the joints. It was also seen in this work that the test temperature had a significant effect on the locus of failure in the joints. At low test temperatures, the failure was found to be predominantly in the composite substrate. As temperature increased, the failure progressed towards cohesive failure of the adhesive. Numerical predictions of the fatigue threshold were carried out using fracture mechanics and stress/strain failure criteria [20]. The effectiveness of a range of failure criteria was evaluated by the ability to predict fatigue thresholds in joints with multidirectional CFRP substrates, using the results from joints with unidirectional substrates to determine the critical failure parameters. Both fracture mechanics and strain-based failure criteria were able to predict the fatigue thresholds to within the experimental scatter for a number of different test environments. In order to develop this work further to predict the strength of a joint with any level of moisture concentration, diffusion analysis coupled to stress and/or fracture analyses is required. As moisture affects the mechanical properties of the adhesive, these properties should be introduced to the stress/fracture analysis model as a function of ageing conditions and test temperature. Also, the changes in moisture concentration during fatigue testing from the steady state conditions should be considered as this affects the mechanical properties of the adhesive. However, before coupling the diffusion and stress analyses, an accurate transient diffusion model is required and this is the subject of this paper.

In this paper, the diffusion of moisture in carbon fibre composite bonded joints is studied experimentally and numerically and analytical solutions for the effect of fillet shape on the diffusion into joints with

impermeable adherends are derived. The paper is divided into six main sections (section 2 to 7). In section 2, the theoretical background to the analytical solution of diffusion problems as well as transient diffusion finite element analysis is presented. In section 3, the experimental results of the water uptake measurements on the adhesive and the unidirectional and multidirectional composites are reported. Closed form solutions for moisture diffusion in metal bonded joints are presented in section 4. This includes a discussion of the effect of a fillet on the diffusion process and the limitations of the closed form solution. In section 5, the results of the finite element diffusion analysis are summarised and the kinetics of moisture distribution within metal and composite bonded joints are studied. The importance of modelling the composite substrate in the diffusion analysis, the effect of the fillet shape and of the substrate type (UD, MD) are investigated. In section 6, a comparison is made between the closed form solution and finite element analysis. Finally, in section 7, experimental results of fatigue tests on lap-strap joints subject to different ageing and testing environments are presented and the correlation between fatigue threshold and moisture content is investigated.

THEORETICAL BACKGROUND TO MOISTURE DIFFUSION IN BONDED JOINTS

Diffusion Equations

Here we briefly summarise the pertinent theory of diffusion and present general equations giving spatial and temporal distributions of diffusant concentration within a regular region with prescribed boundary conditions. We shall go on to see how approximate solutions for more physically meaningful configurations can be generated. Specifically, we shall consider the diffusion of moisture through protective fillets of adhesive formed when manufacturing a bonded joint. In all this work we shall consider the case of Fickian diffusion where the rate of mass transfer/unit area (F_x) in a given direction (x) is taken to be proportional to the gradient of the moisture concentration (c) in that direction, *i.e.*,

$$F_x = -D\frac{\partial c}{\partial x} \tag{1}$$

By considering the total transport of moisture into and out of a control volume we arrive at the rate of change of moisture in the control volume. This is illustrated in Figure 1 and Equation (2):

$$-\frac{\partial F_x}{\partial x}-\frac{\partial F_y}{\partial y}=\frac{\partial c}{\partial t} \tag{2}$$

For simplicity, only two dimensions have been considered but the principle and equations can easily be extended to three dimensions.

By substituting Equation (1) into (2) we arrive at the general governing equation for moisture concentration in two dimensions, *i.e.*,

$$\frac{\partial}{\partial x}\left(D\frac{\partial c}{\partial x}\right)+\frac{\partial}{\partial y}\left(D\frac{\partial c}{\partial y}\right)=\frac{\partial c}{\partial t} \tag{3}$$

In the case that D is independent of direction and the concentration of the diffusant, Equation (3) can be simplified to:

$$D\left(\frac{\partial^2 c}{\partial x^2}+\frac{\partial^2 c}{\partial y^2}\right)=\frac{\partial c}{\partial t} \tag{4}$$

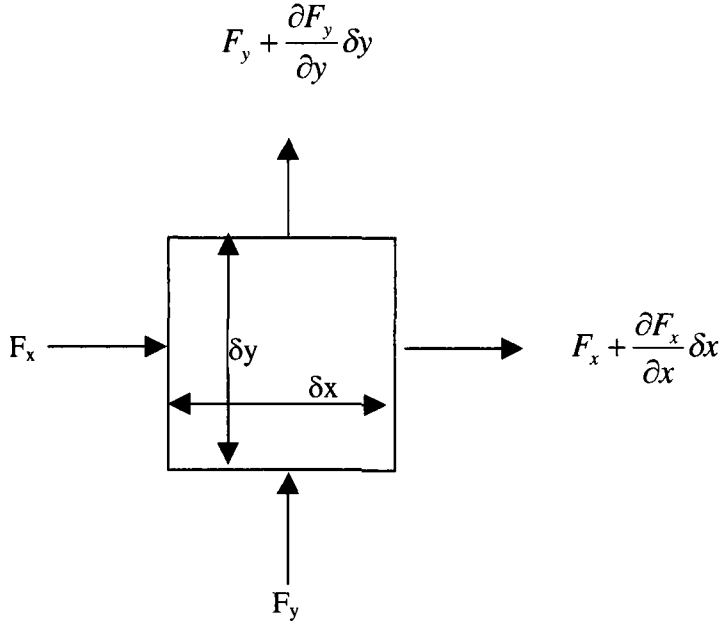

FIGURE 1 Two-dimensional moisture transport.

Anisotropic media, such as the composite adherends discussed later in this paper, may have different diffusion properties in different directions and Equation (1) must be replaced with the following equations.

$$\begin{aligned} -F_x &= D_{11}\frac{\partial c}{\partial x} + D_{12}\frac{\partial c}{\partial y} + D_{13}\frac{\partial c}{\partial z} \\ -F_y &= D_{21}\frac{\partial c}{\partial x} + D_{22}\frac{\partial c}{\partial y} + D_{23}\frac{\partial c}{\partial z} \\ -F_z &= D_{31}\frac{\partial c}{\partial x} + D_{32}\frac{\partial c}{\partial y} + D_{33}\frac{\partial c}{\partial z} \end{aligned} \tag{5}$$

Substitution into the 3-dimensional form of Equation (2) for the case of concentration-independent D gives us:

$$\begin{aligned} D_{11}\frac{\partial^2 c}{\partial x^2} + D_{22}\frac{\partial^2 c}{\partial y^2} + D_{33}\frac{\partial^2 c}{\partial z^2} + (D_{23} + D_{32})\frac{\partial^2 c}{\partial y \partial z} \\ + (D_{31} + D_{13})\frac{\partial^2 c}{\partial z \partial x} + (D_{12} + D_{21})\frac{\partial^2 c}{\partial x \partial y} = \frac{\partial c}{\partial t} \end{aligned} \tag{6}$$

Equation (6) can be simplified by a transformation to orthogonal axes defined by ξ, η and ζ.

$$D_1\frac{\partial^2 c}{\partial \xi^2} + D_2\frac{\partial^2 c}{\partial \eta^2} + D_3\frac{\partial^2 c}{\partial \zeta^2} = \frac{\partial c}{\partial t} \tag{7}$$

where D_1, D_2 and D_3 are the principal diffusion coefficients. In the case of diffusion into thin films of anisotropic media such that the diffusion is essentially one-dimensional, Equation (6) simply reduces to:

$$D_{11}\frac{\partial^2 c}{\partial x^2} = \frac{\partial c}{\partial t} \tag{8}$$

In laminated composites D_{11} in Equation (8) usually corresponds to one of the principal diffusion coefficients.

Analytical Solution

Equation (4) can be solved for a rectangular region in which the concentration is initially zero everywhere and then all boundaries are instantaneously subjected to a constant uniform concentration of c_o, Figure 2.

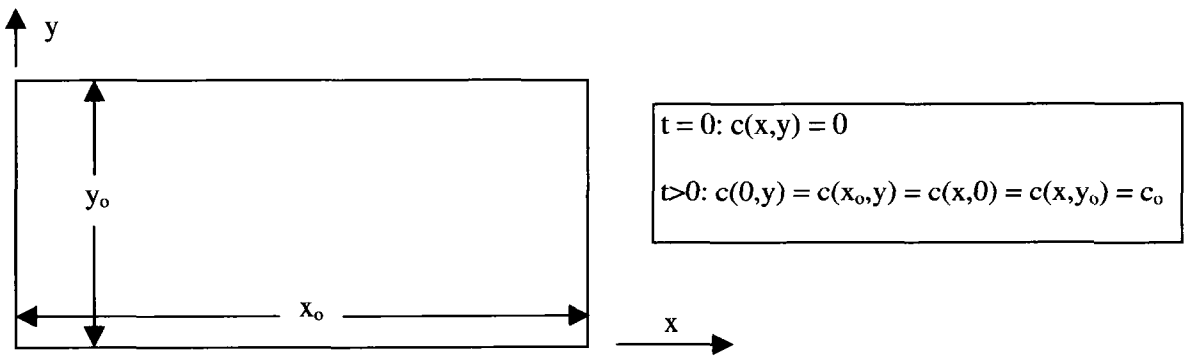

FIGURE 2 Initial and boundary conditions for a rectangular region.

Assuming two-dimensional diffusion in the x and y directions with no flux in the third direction, the solution to Equation (4) can be shown to be [21]:

$$c = c_o - \sum_{j=0}^{\infty}\sum_{m=0}^{\infty} \frac{16c_o}{(2j+1)(2m+1)\pi^2} \sin\left(\frac{(2j+1)\pi x}{x_o}\right) \sin\left(\frac{(2m+1)\pi y}{y_o}\right) e^{[-((2j+1)/x_o)^2-((2m+1)/y_o)^2]D\pi^2 t} \quad (9)$$

This equation can be used directly to evaluate moisture distributions in 2-D plane regions; however, to implement it requires summing two series until convergence is obtained. An alternate approach is to use the fact that for the boundary conditions in question, it can be shown that the solution can be expressed as the product of the 1-D solutions in the coordinate directions, *i.e.*:

$$1 - \frac{c}{c_o} = \left(1 - \frac{c_x}{c_o}\right)\left(1 - \frac{c_y}{c_o}\right) \quad (10)$$

The 1-D solution can be found from Equation (4) as [21]:

$$1 - \frac{c(x,t)}{c_o} = \sum_{j=1}^{\infty} \frac{4}{(2j+1)\pi} \sin\left(\frac{(2j+1)\pi x}{x_o}\right) e^{-((2j+1)/x_o)^2 D\pi^2 t} \quad (11)$$

This, and a similar expression for diffusion in the y-direction, can be substituted into Equation (10) to provide an alternate solution for the 2-D domain.

The problem outlined in Figure 2 can be recast slightly with a new co-ordinate system (α,β) being placed at the centre of the rectangle. For such a system Equations (9) to (11) can be shown to be given by Equations (12) to (14) respectively.

$$c = c_o - \sum_{j=0}^{\infty}\sum_{m=0}^{\infty} \frac{16c_o(-1)^n(-1)^m}{(2j+1)(2m+1)\pi^2} \cos\left(\frac{(2j+1)\pi\alpha}{x_o}\right) \cos\left(\frac{(2m+1)\pi\beta}{y_o}\right) e^{[-((2j+1)/x_o)^2-((2m+1)/y_o)^2]D\pi^2 t} \quad (12)$$

$$1 - \frac{c}{c_o} = \left(1 - \frac{c_\alpha}{c_o}\right)\left(1 - \frac{c_\beta}{c_o}\right) \tag{13}$$

$$1 - \frac{c(\alpha, t)}{c_o} = \sum_{j=1}^{\infty} \frac{4(-1)^j}{(2j+1)\pi} \cos\left(\frac{(2j+1)\pi\alpha}{x_o}\right) e^{-((2j+1)/x_o)^2 D\pi^2 t} \tag{14}$$

Finite Element Method

The analytical solution for moisture diffusion is limited to simple geometry and to linear Fickian analysis [21, 22]. However, the finite element method can be used for more complex geometry, taking into account non-linear effects. As diffusion is a transient phenomenon, transient field analysis is the most appropriate form for finite-element-based diffusion analysis. The moisture concentration calculated from a transient diffusion analysis can subsequently be used as input for stress analysis allowing for the incorporation of moisture-dependent mechanical properties in the model. Transient diffusion finite element analysis is used to determine the normalised moisture concentration, c/c_∞, and other diffusion quantities as a function of time of exposure to a wet environment. The material data required for transient diffusion analysis is the coefficient of diffusion, which is a constant for Fickian models and a function of moisture for some non-Fickian models. In the latter case, the analysis becomes non-linear. In order to enhance the accuracy of the solution small integration time steps should be used. In many FEA packages, the integration time step can be automatically controlled so that it changes based on the response of the model. This response could be evaluated by considering the number of equilibrium iterations used in a previous time step and by calculating the response eigenvalue using the substep solution vector and the diffusion matrix. The smaller the eigenvalue from the present substep the larger the required time step for the next substep and vice-versa. The user can specify an upper and lower limit for time stepping in order to limit the range of variation in time step. The general form of the diffusion differential equation in 3-D can be expressed as:

$$\frac{\partial}{\partial x}\left(D_x \frac{\partial c}{\partial x}\right) + \frac{\partial}{\partial y}\left(D_y \frac{\partial c}{\partial y}\right) + \frac{\partial}{\partial z}\left(D_z \frac{\partial c}{\partial z}\right) = \frac{\partial c}{\partial t} \tag{15}$$

where D_x, D_y and D_z denote the diffusion coefficients in the x, y and z directions. Transient finite element analysis is required in order to solve this diffusion differential equation [23, 24]. The classical procedures of the finite element method are followed in the solution of this equation allowing for complex geometry or boundary conditions. These procedures are a) divide the solution domain into small finite elements, b) define the variation of the field variable (the normalised moisture concentration, c/c_∞) by suitable shape functions, c) use a variational approach to derive the element matrix, d) assemble the element matrices, e) apply boundary conditions and time stepping and f) solve the equations at each time step. After obtaining the solution, the results can be reviewed for the entire model at a specific time or for a specific point in the model over the entire time.

EXPERIMENTAL PROGRAM

In order to model the diffusion of water into adhesively bonded CFRP joints, it is essential to have sorption kinetics data for the substrate and the adhesive in the environment being modelled. This is usually generated experimentally by measuring the change in mass of a sample of material in an environment of controlled temperature and relative humidity (RH) on absorption (or desorption) of water. A relevant diffusion model can then be fitted to the data to extract the diffusion constants.

Water sorption data for the adhesive and CFRP are presented in this section. The materials used in this study were those used in recent investigations of the effect of environment on the fatigue of composite joints [18 – 20]. The adhesive used was a proprietary, modified epoxy, which was supplied as 0.2mm film with a non-woven nylon carrier. The adhesive was based on a diglycidyl ether of bisphenol A epoxy, crosslinked with a primary amine curing agent. A reactive liquid polymer, based upon a carboxyl-terminated butadiene acrylonitrile rubber, was used as a toughening agent. The formulation also contained a silica filler. The adhesive was cured for 60 minutes at 120°C. The CFRP had a modified bismaleimide/epoxy matrix and intermediate modulus carbon fibre reinforcement. The pre-preg material was laid up as unidirectional (16 ply at 0°) or multidirectional

$[(0°/-45°/+45°/0°)_2]_S$ panels and was cured at 182°C for 2 hours, with an initial autoclave pressure of 0.6 MPa.

Absorption was measured at 45°C/85% RH and at 90°C/97% RH. The former is the environment in which the joints were conditioned and the latter represents the conditions in the environmental chamber when the joints were tested "hot/wet". In addition, desorption has been observed at 90°C and ambient humidity for the CFRP, as this represents the condition when aged joints were tested at high temperatures in "dry" conditions.

Moisture Diffusion in Adhesive Films

Although several mechanisms of water penetration in adhesives have been proposed, it is generally accepted that diffusion represents the most important of these. If water enters a joint by diffusion through the adhesive, and the diffusion is restricted to the x-direction, then the uptake for the case of concentration-independent diffusion can be described by Equation (4). The solution for the case of an initially dry, thin film of adhesive immersed in water, or water vapour at a constant partial pressure, is given by Equation (11). The total weight of moisture is obtained by integrating c(x,t) over the adhesive thickness, l (where x_0 is equivalent to l), *i.e.*:

$$M = A \int_0^l c\,dx \tag{16}$$

where A is the exposed surface area. The result of the integration provides the total mass uptake by the film at time "t".

$$\frac{M_t}{M_\infty} = 1 - \sum_{j=0}^{\infty} \frac{8}{(2j+1)^2\pi^2} e^{[((-2j+1)^2\pi^2 Dt)/l^2]} \tag{17}$$

M_t is the mass of water absorbed at time "t" and M_∞ is the mass of water absorbed at equilibrium. At short times, Equation (17) may be simplified to:

$$\frac{M_t}{M_\infty} = \frac{4}{l}\left(\frac{Dt}{\pi}\right)^{\frac{1}{2}} \tag{18}$$

The ratio M_t/M_∞ is known as the fractional uptake. The diffusion coefficient, D, can be deduced from the initial slope of an M *versus* $\sqrt{t}$ curve, since:

$$D = \pi\left(\frac{l}{4M_\infty}\right)^2\left(\frac{M_2 - M_1}{\sqrt{t_2} - \sqrt{t_1}}\right)^2 \tag{19}$$

A plot of the mass uptake against the square root of time represents the Fickian diffusion curve for the adhesive. A good fit of the experimental data with this curve would, therefore, confirm the applicability of a Fickian diffusion model for the material considered. It has been noted with epoxy resins that water uptake becomes increasingly non-Fickian as humidity and temperature increase [5]. In order to compare moisture uptake in films of different thickness the $\sqrt{t}$ term should be replaced with $\sqrt{t}/l$. The fractional mass uptake is then plotted against $\sqrt{t}/l$ and the diffusion coefficient, D, for the linear region of water uptake calculated using Equation (19). Such graphs are known as uptake or sorption plots. The linear portion of the uptake plot usually extends up to $M_t/M_\infty \cong 0.6$. A measure of the solubility of a liquid in an adhesive can be expressed by the parameter c_∞, which is defined as the concentration of the liquid absorbed at equilibrium. The ability of an adhesive to transmit water (or any other fluid) will, therefore, depend upon the diffusion coefficient, D, and the solubility coefficient, c_∞. The product of the diffusion and solubility coefficients defines the permeability coefficient, Dc_∞.

Thin adhesive films for the sorption experiments were prepared by first removing sheets of the adhesive from a freezer and storing under vacuum at $\sim 40°C$ to degas. This process was carried out for a minimum of two days prior to curing. The cure cycle was 120°C for 60 minutes, with a bonding pressure of 170 kPa. The temperature at the bondline was monitored using a calibrated thermocouple in order to ensure the correct curing conditions were achieved. Moisture uptake samples approximately 10 mm in diameter were cut out from the 0.2mm cured sheets using a die-cutter. These samples were dried to constant mass over phosphorous pentoxide (P_2O_5) to ensure negligible water content before conditioning. The diffusion coefficient was calculated from measurements made on an environmental micro-balance. The dried samples were conditioned in a sealed balance head

of the two pan type, with distilled water providing the required humidity. The whole balance head was further enclosed in a large heated chamber in order to maintain a constant temperature. Mass increase was recorded continuously on a chart recorder. Three samples were tested in each environment and additional data on the equilibrium moisture content were obtained by conditioning samples in environmental chambers and removing them periodically for mass measurement on a Mettler AE160 balance.

Typical plots of M_t/M_∞ against $\sqrt{t}/l$ are shown in Figure 3 for adhesive samples conditioned at 45°C/85% RH and 90°C/97% RH, respectively. It can be seen that approximately Fickian behaviour is observed for the adhesive at both conditioning environments. As expected, the rate of diffusion was greater at the higher temperature. More scatter is seen in the moisture uptake plot at 90°C/97% RH and difficulties were experienced in operating the microbalance in these conditions.

Moisture Diffusion into Composite Materials

For a composite sample in which diffusion is restricted to the x-direction, moisture sorption is described by Equation (8). The solution to this equation will be of the form described by Equation (11) with D substituted by D_x to account for the directional dependence

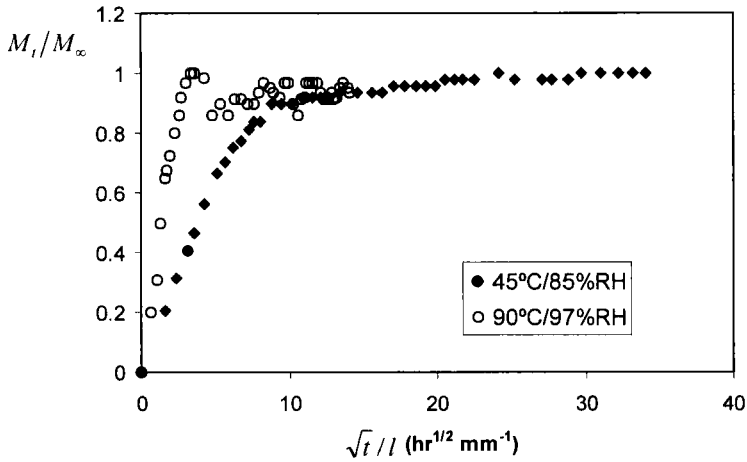

FIGURE 3 Water uptake plots for adhesive.

of the diffusion constant in composite materials. We can then use the same arguments used in Section 3.1 to derive an expression similar to Equation (17) (with $D_x = D$) to describe the mass uptake as a function of time.

Assuming that the material exhibits Fickian behaviour, the diffusivity, D, may be calculated from the linear portion of a M *versus* $\sqrt{t}$ plot using Equation (19). If moisture entering from the edges can be neglected then $D_x = D$ and the value calculated from Equation (19) can be substituted directly into Equation (17) in order to calculate the moisture content at any time, t. If water absorption at the sample edges cannot be ignored then the three-dimensional form of Equation (12) needs to be integrated over the sample volume to obtain the expression describing the variation in mass uptake with time.

$$\frac{M_t}{M_\infty} = 1 - \frac{512}{\pi^6} \sum_{i=0}^{\infty} \sum_{j=0}^{\infty} \sum_{k=0}^{\infty} \frac{e^{[-(2i+1)^2\pi^2(D_x t/l^2)]}}{(2i+1)^2} \frac{e^{[-(2j+1)^2\pi^2(D_y t/m^2)]}}{(2j+1)^2} \frac{e^{[-(2k+1)^2\pi^2(D_z t/\ln^2)]}}{(2k+1)^2} \tag{20}$$

where l, m and n are the dimensions of the sample in Equation (20). An alternative to fitting the full three-dimensional equation given above is to use an edge-correction technique and a number of these have been suggested in the literature [25, 26]. In this work, however, the data are fitted to the 3-dimensional model given in Equation (20) when Fickian uptake is observed. This is achieved by using the numerical curve-fitting method described by Bond [27], which is based on the Levenberg-Marquardt technique. In the case of obviously non-Fickian uptake, an estimate of the diffusion coefficient in the early stages of diffusion was determined from the initial slope of the sorption plot using Equation (19). This is obviously a less rigorous method of analysing the data, however, it is considered to be suitable for the purposes of the current work as long as the approximate nature of the subsequent predictions of moisture uptake in the conditions exhibiting anomalous uptake are acknowledged.

The composite sheets for the sorption studies were prepared using either UD [0°] or MD $[(0°/-45°/+45°/0°)_2]_S$ panels. 50 mm × 50 mm × 4 mm samples were cut from the composite panels for the absorption and desorption studies. Absorption at 45°C/85% RH and

at 90°C/97% RH was achieved by ageing in an environmental chamber. The weight changes were determined throughout the ageing period using a Mettler AE160 balance and recorded as a function of ageing time. No fixed time interval was used to conduct the weighing but a sliding scale was adopted to follow the relationship of moisture uptake with the square root of exposure time. For the desorption study, samples which had reached equilibrium at 45°C/85% RH were transferred to an oven set at 90°C. Throughout the desorption study, the samples were removed from the oven, allowed to equilibrate thermally to laboratory conditions and weighed using a Mettler AE160 balance. The weight change of the specimens was plotted as a function of ageing time, as in the absorption studies.

Average uptake plots for the MD and UD samples conditioned at 45°C/85% RH are shown in Figure 4. The sorption uptake profiles for the unidirectional composite are essentially Fickian. The results from the water uptake studies conducted on the MD samples, however, appear to exhibit a degree of anomalous behaviour. This difference in water uptake may be due to the different laminate configurations and the effect this has on the ability of the matrix to expand and absorb additional moisture.

Figure 5 shows the absorption plots for the CFRP at 90°C/97% RH. Water uptake is obviously non-Fickian in these conditions and equilibrium has not been reached at the end of the conditioning

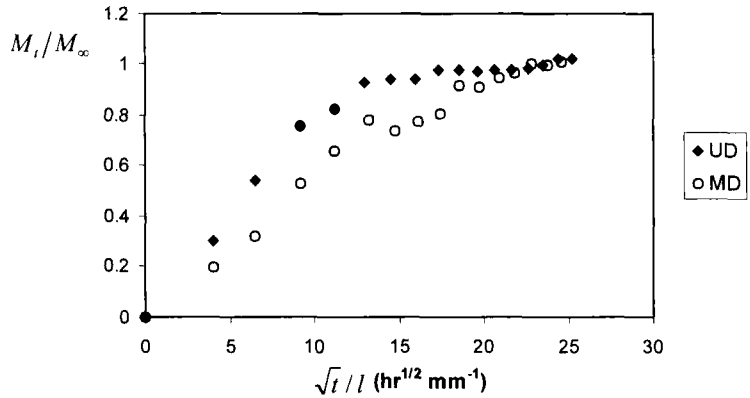

FIGURE 4 Water uptake plots for the CFRP at 45°C/85% RH.

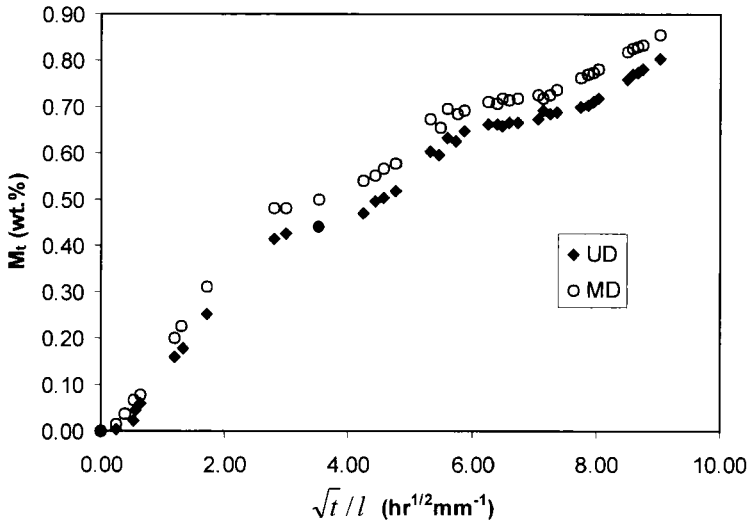

FIGURE 5 Water uptake plots for the CFRP at 90°C/97% RH.

period. The deviation from Fickian behaviour may be attributable to secondary relaxation processes as the glass transition temperature of the polymeric matrix approaches the ageing temperature. Alternatively, the anomalous uptake profiles may be associated with the internal equilibration between bound and free penetrant molecules. The increasing relaxation and reorganisation of the network freeing additional bonding sites for moisture interaction resulted in dual sorption behaviour being observed. It can also be seen in Figure 5 that there is no significant difference between the water uptake profile for the UD and MD samples, hence, fibre direction does not significantly affect the water diffusion characteristics of the composite material in this environment. Bond [27] also observed that Fibre Reinforced Composite (FRC) lay up configuration did not have a significant effect on the water diffusion characteristics of T800/924 composite material, when studied under high temperature/high activity environments.

Desorption plots for the CFRP at 90°C/ambient humidity are shown in Figure 6. Fickian behaviour is observed and there is little difference between samples with the MD and UD lay-ups. This may be expected because the desorption process does not need to await relaxation effects and, hence, less anomalous behaviour is observed.

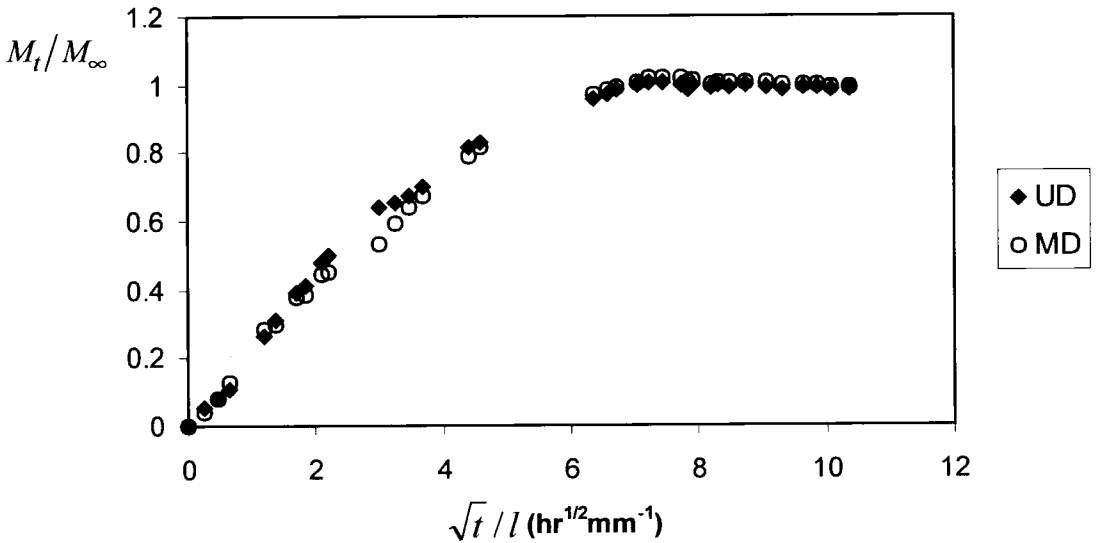

FIGURE 6 Desorption plots for the CFRP at 90°C/ambient humidity.

Determination of Diffusion Coefficients and Equilibrium Moisture Content

The water uptake data for the adhesive from the microbalance measurement were entered into a computer programme that fitted a 1-D Fickian curve to the data and computed D and M_∞. The coefficients of diffusion obtained from these plots are presented in Table 1. The M_∞ values in the table are an average of those from the microbalance measurement and from samples aged in environmental chambers. In the table a range of values is given for M_∞ for the adhesive conditioned at 90°C/97% RH. This is because in some cases a secondary uptake stage was observed, leading to a higher equilibrium moisture content.

The sorption profiles for the UD CFRP conditioned at 45°C/85% RH exhibited Fickian behaviour and a 3-D Fickian curve-fitting program was used to determine D and M_∞. As the sorption plot for the MD CFRP in this environment exhibited some anomalous behaviour, the diffusion coefficient was determined by using the Fickian curve-fitting programme and also from the slope of the initial linear portion of the plot of M_t/M_∞ against $\sqrt{t}/l$. The results obtained from the 90°C/97% RH sorption studies showed that Fickian behaviour was not observed under the high temperature/high activity ageing conditions. In this case, fitting a Fickian curve to the data would be meaningless; therefore, an estimate of D in the early stages of absorption was determined from the slope of the initial linear portion of the plot of M_t/M_∞ against $\sqrt{t}/l$. The desorption profiles exhibited

TABLE 1 Summary table of diffusion constants

Material	*Conditioning environment*	*D* (10^{-13} m^2s^{-1})	M_∞ (*wt. %*)	*Data reduction*
Adhesive	45°C/85% RH-absorption	9.3	1.9	F
CFRP (UD)	45°C/85% RH-absorption	3.6	0.44	F
CFRP (MD)	45°C/85% RH-absorption	1.3	0.40	F
CFRP (MD)	45°C/85% RH-absorption	1.9	0.40	S
Adhesive	90°C/97% RH-absorption	72	1.5-4.4	F
CFRP (UD)	90°C/97% RH-absorption	79	> 0.8	S
CFRP (MD)	90°C/97% RH-absorption	62	> 0.8	S
CFRP (UD)	90°C/ambient-desorption	22	0.66	F
CFRP (MD)	90°C/ambient-desorption	21	0.64	F

F = D calculated from Fickian curve fit to complete data set.
S = D calculated from initial slope of water uptake plot.

Fickian behaviour and, therefore, the curve fitting routine was used to determine the diffusion coefficient of the samples.

DIFFUSION IN BONDED JOINTS: CLOSED FORM SOLUTIONS

When a bonded joint is manufactured, excess adhesive often forms in fillets at the end of the overlaps. It has been acknowledged for some time that these are advantageous in a structural sense as they transfer some of the load. This reduces the value of the peak stress at the end of the overlap and in so doing strengthens the joint. It is also apparent that they are useful when the joint is exposed to a hostile wet environment. Before the moisture can degrade the most highly stressed adhesive at the end of the overlap it needs to pass through the fillet, which effectively serves as a diffusion retarder. In order to be able to assess the retarding effect of the fillet a number of approximate diffusion analyses have been carried out and these are discussed below.

Figure 7 shows the different ways of modelling the adhesive fillet, along with the pertinent geometry. Each will be considered in turn for the case of an adhesively bonded joint with impermeable adherends. In each case the accuracy of the results relies on the thickness of the adhesive layer being small in relation to the characteristic fillet size. In most practical situations this will not impose a severe limitation.

a) Radiused Fillet

As there is no flux across the horizontal and vertical boundaries in the fillet the ensuing moisture diffusion is axisymmetric in nature and is governed by the following equation:

$$\frac{\partial c}{\partial t} = \frac{1}{r}\frac{\partial}{\partial r}\left(rD\frac{\partial C}{\partial r}\right) \tag{21}$$

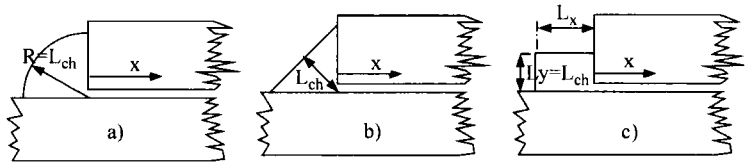

FIGURE 7 Adhesive fillet models.

This can be solved by the method of separating the variables to give the concentration as a function of time, t, and position, r, in the fillet. The case of an initially dry fillet that instantaneously reaches full saturation (c_∞) on the outer surface yields the following distribution.

$$\frac{c}{c_\infty} = 1 - \frac{2}{R}\sum_{n=1}^{\infty} \frac{J_o(r\alpha_n)e^{-Dt\alpha_n^2}}{\alpha_n J_1(R\alpha_n)} \tag{22}$$

Here J_o and J_1 are Bessel functions of zero and first orders, respectively, with arguments of $r\alpha_n$ and $R\alpha_n$, respectively, and α_i are the roots of $J_o(R\alpha_i) = 0$. From this the variation in concentration with time at the centre of the zone ($r = 0$) can be determined and this is shown graphically in Figure 8. It can be seen that the concentration rises in a decaying manner to the saturated value, as expected. Knowing the coefficient of diffusion of the adhesive and the fillet radius it is possible to use this figure (or Equation (22)) to determine the time taken to reach a certain moisture concentration and, hence, assess the retarding effect of the fillet. A useful comparison can be made against the predictions obtained by assuming 1-D diffusion with the path length set as the shortest path, in this case the radius of the

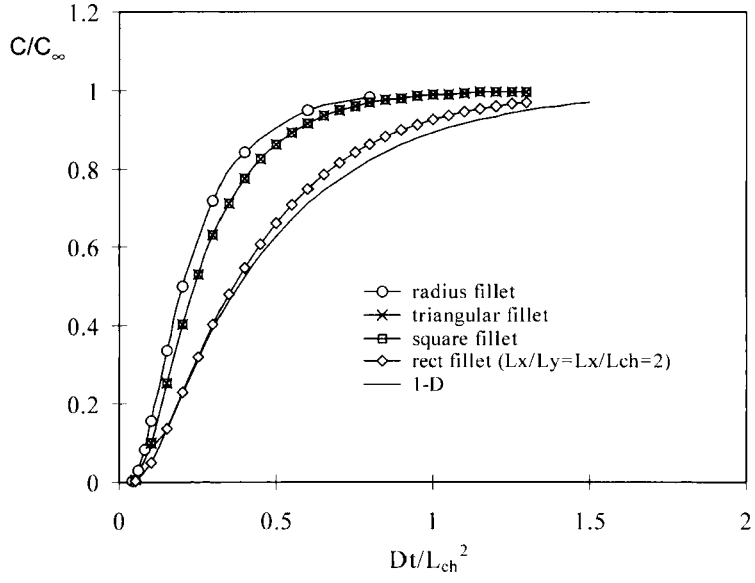

FIGURE 8 Moisture concentration *versus* time from different fillet shapes.

fillet R. These data are also shown on Figure 8. It can be seen that using a 1-D model with the characteristic length (semi-film thickness) equal to the radius significantly overestimates the retardation effect of the radiused fillet. The reason for this is that the moisture flows into the fillet all around its perimeter but all this is directed towards the centre at the overlap end. This channelling actually delivers more moisture than simple 1-D diffusion.

b) Triangular Fillet

Diffusion in the 45° triangular fillet as (seen in Figure 7b) can be found by considering the diffusion into a square plate as seen in Figure 9. In a joint no moisture would cross the diagonals OX and OY and this is precisely the case for a square plate subjected to a constant concentration on all 4 sides.

Any of the approaches given in Equations (4) to (9) can be used to determine the spatial and temporal moisture distribution within a square plate. This has been done and the resulting distribution of concentration with time at O (the end of the adhesive overlap) is given in Figure 8. It can be seen that the retardation effect is slightly higher than that of the radius fillet of the same characteristic length (the same as the shortest path in both cases). This is because although the shortest path is the same in both cases, in the fillet the path length from the periphery to the overlap end (where the moisture concentration is calculated) increases as the point moves towards either substrate and, thus, the moisture transport process from these positions takes longer.

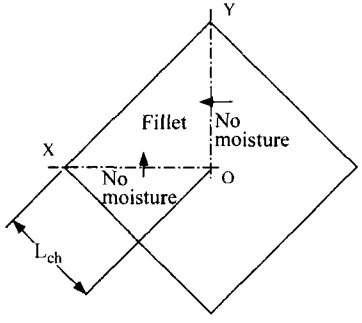

FIGURE 9 Diffusion in a square plate.

Again, the 1D calculation based upon shortest path length still significantly overpredicts the retarding effect of the triangular fillet.

c) Rectangular Fillet

Although not such an aesthetically pleasing shape, the rectangular fillet often occurs as part of a hot-pressing manufacturing process; indeed, it was found on a number of the joints reported later in this paper. Taking the height of the fillet, L_y, as the characteristic length, L_{ch}, the variation of moisture at the overlap end ($x = 0$) can be found from the 2-D diffusion Equations (9 – 14). The data so generated are shown in Figure 8. Note that the triangular and square fillets, with the characteristic lengths as defined in Figure 7, have the same temporal variation of moisture concentration. As the fillet becomes more rectangular, the diffusion profile approaches that of the 1-D model. This is because the moisture transport direction to the overlap end becomes predominantly orientated in the vertical (L_y) direction.

FINITE ELEMENT ANALYSIS

The lap-strap joints (see Section 7) conditioned in a humid environment were stored in a humidity chamber at 45°C/85% RH prior to testing. The joints were weighed at different intervals to monitor water uptake until equilibrium was reached. Approximately one year was required to reach saturation. In this section, a finite element diffusion analysis is carried out in order to study and understand the moisture transport in the joint. In the first instance, the effect of the composite substrates on the moisture diffusion in the adhesive layer is studied. Next, a comparison between the diffusion process in the UD and MD is presented. Finally, the effect of using tapered fillet (rather than a square) on the moisture concentration is reported.

The lap-strap configuration and dimensions are shown in Figure 10. Initially, the effect of modelling the composite in the diffusion analysis will be investigated. Because the diffusion coefficient of the adhesive is normally one order of magnitude higher than that of the composite, one might expect a minor effect from modelling the composite. In order to investigate this effect, two diffusion finite element analyses are

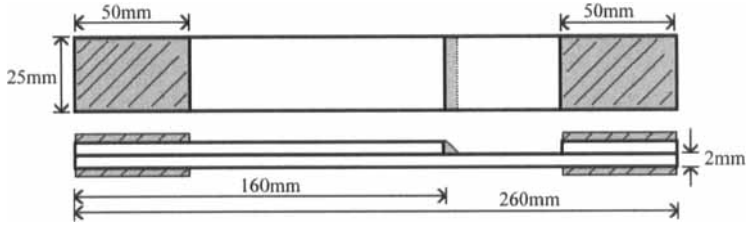

FIGURE 10 Lap-strap joint.

performed. In the first analysis, only the adhesive layer and the fillet are modelled, whilst in the second one the whole assembly is modelled, *i.e.*, composite, adhesive and fillet. The finite element meshes at the overlap end for these two analyses are shown in Figure 11. In the first analysis, a fully-saturated boundary condition is applied at the exposed edges of the adhesive and fillet, whilst a moisture concentration gradient equal to zero is applied to the other edges (edges adjacent to composite). In the second analysis, all edges (composite, adhesive and fillet) are assumed to be saturated (all edges are exposed). It should be noted that the first analysis corresponds to the case of a bonded metal joint, as no diffusion through the substrate sides is assumed. The diffusion coefficient used in these analyses for the adhesive is the one measured at 45°C/85% RH and for the composite is the one measured at 45°C/85% RH for the UD laminate (see Table 1). These coefficients of diffusion of the adhesive are considered as a good representative value for the hot/wet ageing as Fickian behaviour is observed in the absorption plots for both adhesive and UD composite in this environment.

The distribution of moisture concentration along the centre of the adhesive layer is plotted in Figure 12 after three different exposure times, 10, 20 and 30 days. The left-hand fillet edge is located at distance "0". The abbreviation "adhv" indicates the first analysis, while "adhv+comp" the second one. A plot of moisture concentration at distances of 1.1 and 2.3 mm from the adhesive edge as a function of exposure time is shown in Figure 13. As the diffusion coefficient of the composite is an order of magnitude less than that of the adhesive, there is some dissipation of moisture from the adhesive layer to the composite when modelling diffusion in both adhesive and composite (analysis 2). It can be concluded that the first analysis (diffusion in

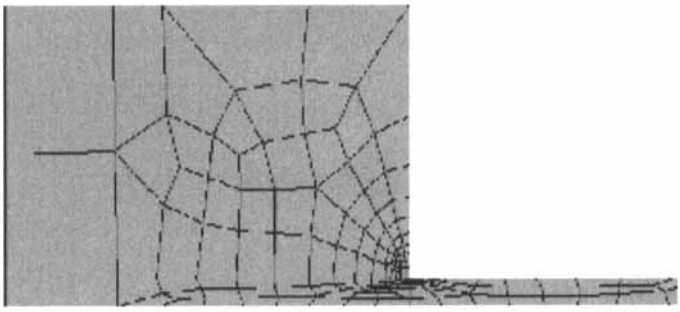

(a) Adhesive

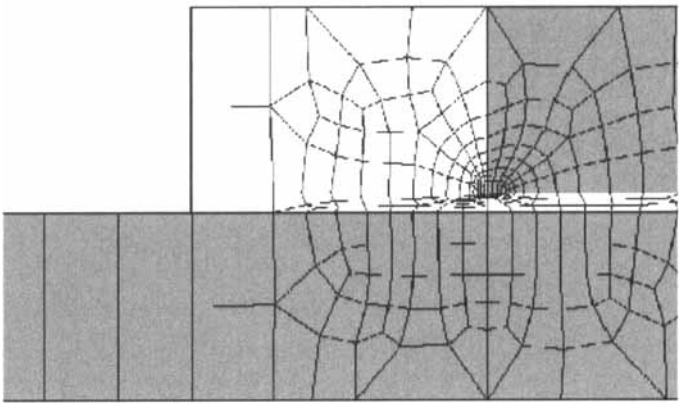

(b) Adhesive+composite

FIGURE 11 Finite element meshes—Diffusion analysis.

adhesive only) results in higher moisture concentration near the adhesive edge during the first month due to the moisture dissipation to the composite in the second analysis. At a distance of 4mm (the end of the lap adherend adjacent to the fillet), there is a clear change in the trend of the curves in Figure 12 due to the geometric and material discontinuity. From a distance of 5mm, the moisture concentration is almost zero in the first analysis indicating that a large part of the adhesive layer is still dry. By contrast, in the second analysis after 20 days, moisture has diffused into the adhesive layer *via* transport through the composite adherends.

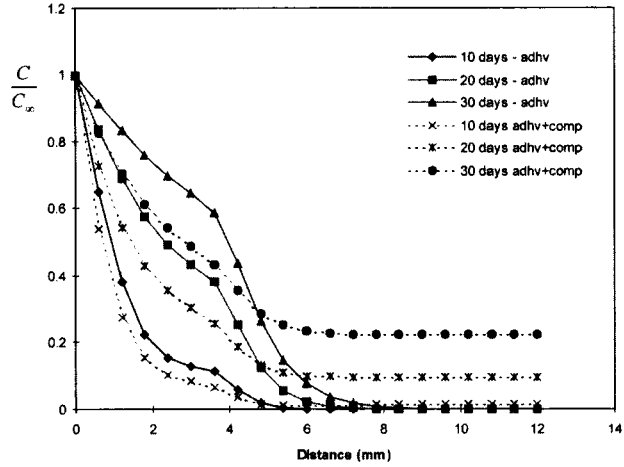

FIGURE 12 Variation of moisture concentration along the adhesive layer.

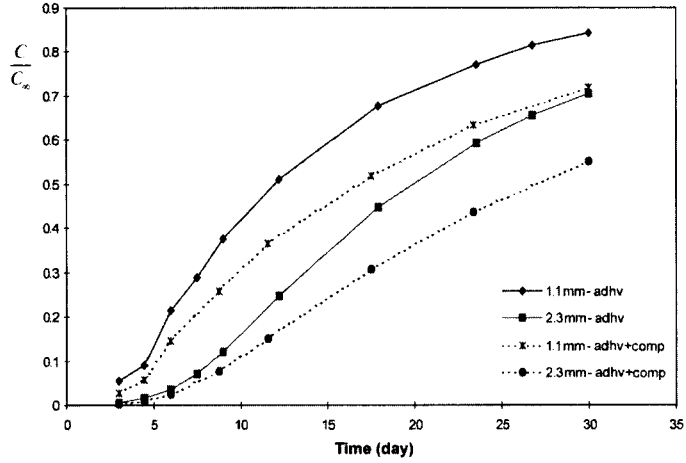

FIGURE 13 Moisture concentration *versus* time (one month).

After one year, the composite becomes fully saturated and delivers more moisture to the adhesive layer as illustrated in Figure 14. The moisture concentration along the adhesive layer computed from analysis 2 is much higher than that computed from analysis 1. In Figure 15, the moisture concentration at a distance of 4 and 10.9 mm from the adhesive fillet edge during the whole exposed period is

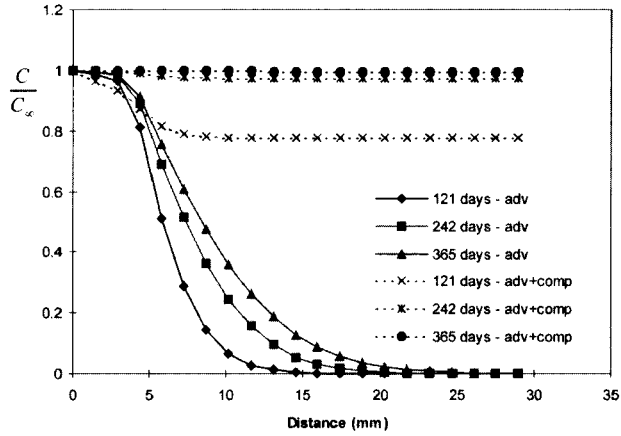

FIGURE 14 Variation of moisture concentration along the adhesive layer.

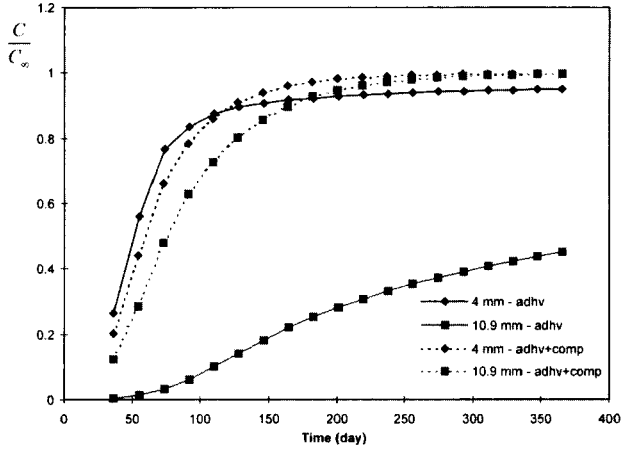

FIGURE 15 Moisture concentration *versus* time (one year).

plotted. Again, it can be seen that the effect of modelling the composite is more pronounced at distances greater than 5 mm from the adhesive edge. After one year, analysis 2 (adhv + comp) suggests that the adhesive layer is fully saturated, whilst analysis 1 (adhv) still predicts a large dry area at the centre of the layer. The results in Figure 15 show that at a distance of 4 mm from the adhesive edge and during the first 100 days, there is moisture dissipation to the composite. After this

period, the adhesive layer gains moisture from the composite. At a distance of 10.9 mm, the moisture concentration in the adhesive layer is completely dominated by the composite. Clearly, modelling the composite is very important in computing the moisture concentration distribution in the adhesive layer. This effect becomes more important at long exposure times after the composite has become saturated with moisture. The comparisons in Figures 12 to 15 can be regarded as comparisons between the diffusion in bonded metal joints (analysis 1) and composite joints (analysis 2) when there is no accelerated diffusion in the interfacial region.

The next step in the FEA diffusion analysis was to investigate the effect of the substrate type (UD/MD) and the fillet type (rectangular or triangular fillet) on the moisture diffusion process. The diffusion coefficients used in this investigation are those measured at 45°C/85% RH and are listed in Table 1. The model of the tapered fillet at the edge of the adhesive layer has an angle of 45°. It should be noted here that the tapered and rectangular fillet models represent the extremes seen in the experimental samples. This can be understood by visualising the autoclave curing process in which the panels to be bonded are layed up on a flat bed with spacing panels, leaving a space at the end of the lap adherend equivalent to the rectangular fillet. The fillet size and shape depend then on how much of this space is filled on curing by spew of the adhesive, the rectangular fillet being the maximum possible size and the tapered fillet representing the smallest fillet seen in practice. The finite element mesh of the tapered fillet joint is shown in Figure 16.

A comparison of the normalised moisture concentration variation along the centre of the adhesive layer after 121 days is shown in Figure 17. The overlap end is located at 4mm on the X-axis. The discontinuity that occurs here results in a change of slope in the concentration profile, Figure 17. The normalised moisture concentration in UD joints is much higher than that in the MD joints owing to the difference in the coefficient of diffusion (UD has a higher coefficient of diffusion than MD, see Table 1). Between the end of the overlap and a distance of about 3mm into the overlap, there is a transition zone in which the contribution of the adhesive fillet and the composite to the moisture distribution interact. Beyond this point, the moisture diffusing from the composite is dominant and flat curves are obtained. A comparison of the moisture concentration at the corner

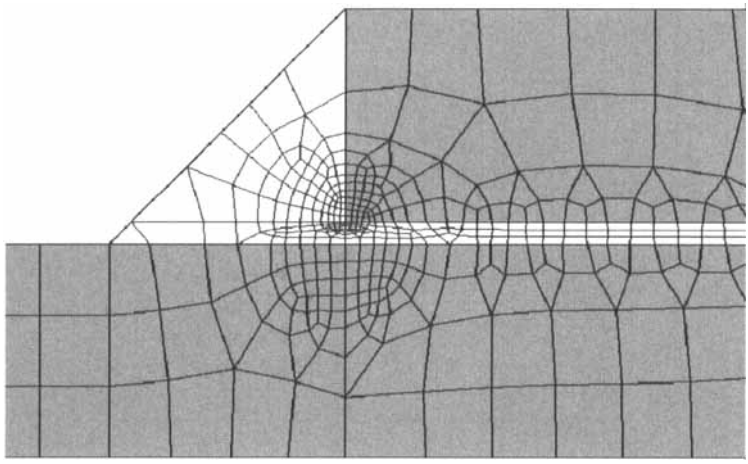

FIGURE 16 F.E. mesh—Tapered fillet.

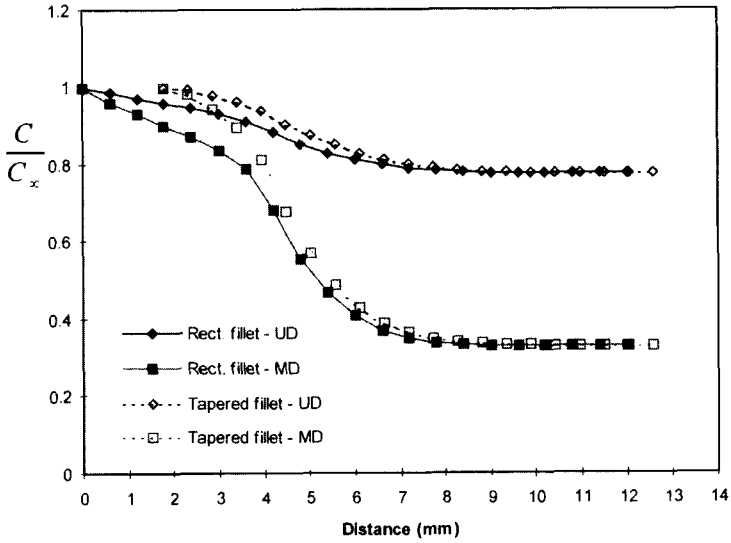

FIGURE 17 Comparison of moisture distribution after 121 days.

point as a function of exposed time is shown in Figure 18. During the early stages of exposure the effect of the tapered fillet is more pronounced. The moisture concentration at the embedded corner of

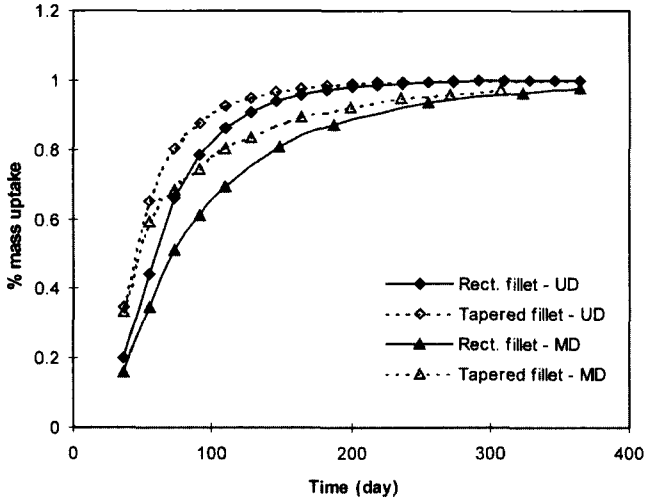

FIGURE 18 Moisture concentration at the corner point.

the lap adherend in the tapered fillet model is much higher than that in rectangular fillet model. This can be attributed to the shorter distance between the exposed edge and the corner point in the tapered fillet joint. After longer exposure time, the transition zone, as well as the composite, becomes fully saturated and the difference of mass uptake between the rectangular and the tapered fillet joints becomes smaller. As can be seen from Figure 18, saturation will be reached at approximately the same time for joints with either rectangular or tapered fillets. Obviously, the MD joints will take a longer time to reach saturation than the UD joints because of the lower diffusion coefficient of the MD substrate.

COMPARISON OF FE AND ANALYTICAL SOLUTION

The analytical solution presented in Section 4 takes into account the moisture transport only in the fillet. It ignores moisture diffusion into the adhesive layer, *i.e.*, assuming that $L_{ch} \gg t_a$ (where L_{ch} is the fillet length as defined in Figure 7, and t_a is the adhesive layer thickness). In order to verify the effect of this assumption on the diffusion profile in the joints, finite element solutions for various adhesive thicknesses

(0.05 mm, 0.1 mm and 0.2 mm) were obtained. For the rectangular fillet, a finite element mesh similar to that shown in Figure 11 a was used, while for the triangular fillet the one shown in Figure 16 (modelling only the adhesive) was used. The results obtained from FEA in the form of moisture concentration at the corner point (C/C_∞) against the dimensionless time parameter (Dt/L_{ch}^2) are compared with those obtained from the analytical solution in Figures 19 and 20 for the rectangular fillet and the triangular fillet, respectively. The finite element solution for the case of $t_a = 0$, which corresponds to modelling only the fillet, is given in Figures 19 and 20, for convenience. As the adhesive thickness increases, the moisture concentration calculated using FEA at the corner point takes a longer time to reach saturation than that calculated using the analytical solution. This is due to the fact that increasing t_a leads to more moisture dissipation into the adhesive layer just below the corner point and causes a larger retardation effect. Therefore, one can conclude that the smaller the adhesive layer thickness, the closer the analytical solution to the FE results.

In order to fit the FEA results for different adhesive thicknesses into the analytical solution a correction factor is proposed. The values of this correction factor are shown in Figure 21. Multiplying the FEA curves in Figure 19 or Figure 20 by the corresponding correction factor, a curve approximated to the analytical solution is obtained.

DIFFUSION IN LAP-STRAP JOINTS TESTED IN FATIGUE

Conditioned and unconditioned lap-strap joints have been tested in fatigue in a variety of environments [19]. A fatigue threshold was defined as the maximum load the samples could withstand without displaying any optically visible damage after 10^6 cycles. Table 2 shows a summary of the results of samples tested at 90°C.

The dry-stored samples were conditioned in a vacuum dessicator at 50°C prior to testing and the wet-stored samples were conditioned in an environmental chamber at 45°C/85% RH until equilibrium, as indicated by constant mass. The "dry" testing was at ambient humidity and the "wet" testing was in a sealed chamber over distilled water. It can be seen that moisture affects the fatigue threshold when

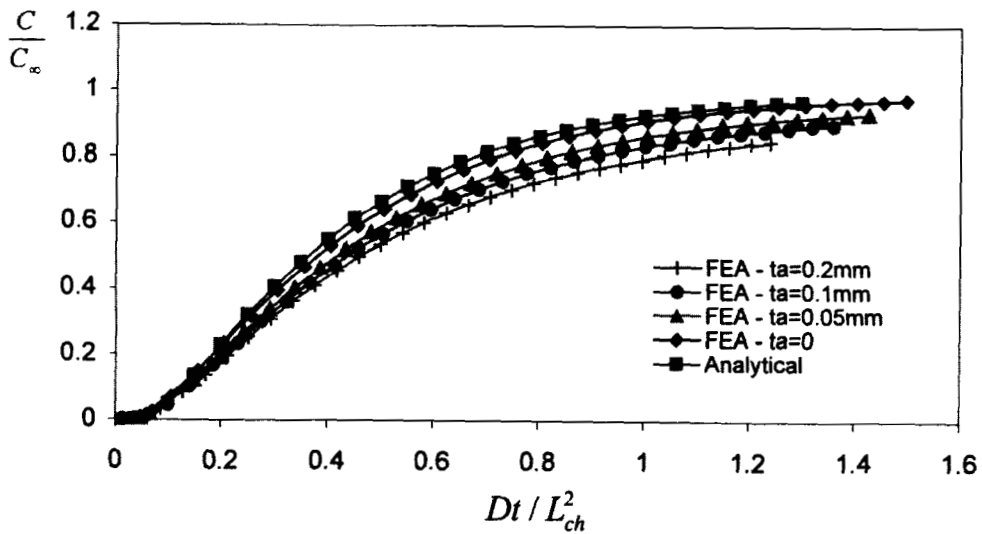

FIGURE 19 Comparison between analytical and FEA—Rectangular fillet.

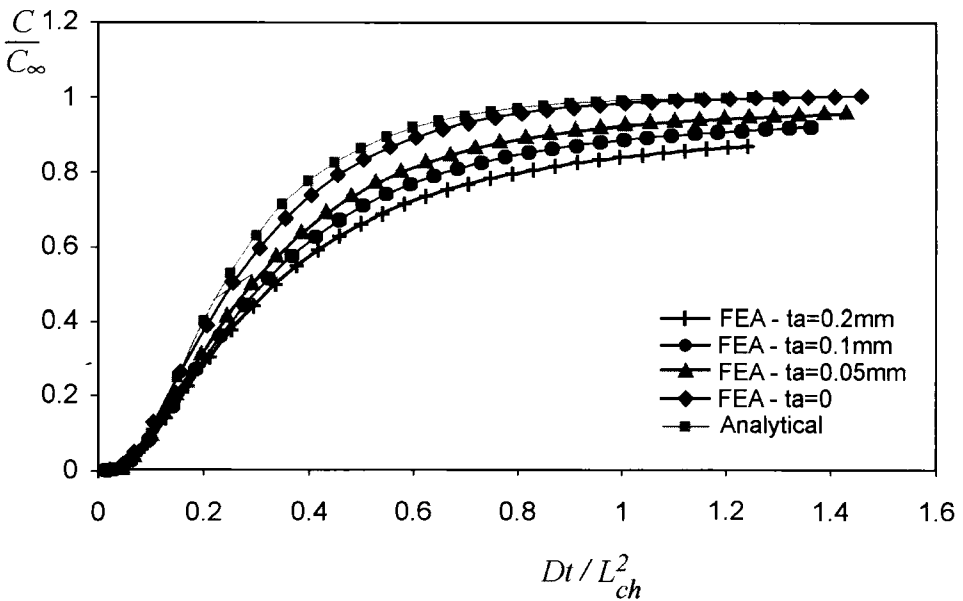

FIGURE 20 Comparison between analytical and FEA—Triangular fillet.

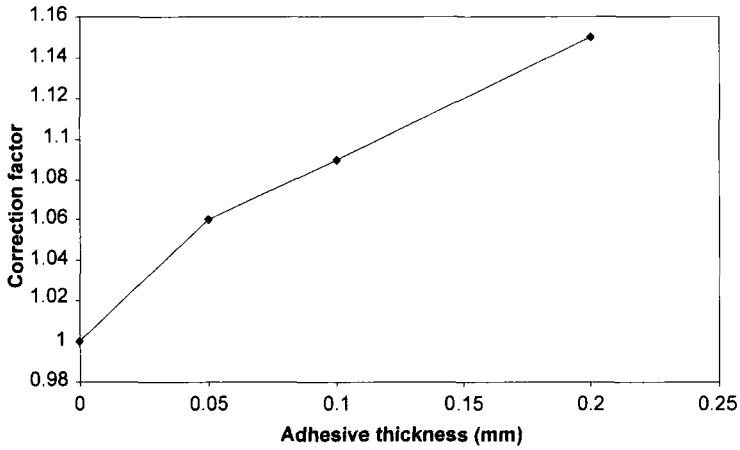

FIGURE 21 Correction factor *versus* adhesive thickness.

TABLE 2 Results of fatigue tests on lap-strap joints

Conditioning	*Test*	*Fatigue threshold load, kN*	
Environment	*Environment*	*UD CFRP*	*MD CFRP*
Stored dry	90°C/dry	14	9
Stored dry	90°C/wet	7	6
45°C/85% RH	90°C/dry	5	4.5
45°C/85% RH	90°C/wet	5	4.5

testing at 90°C. The diffusion of moisture into or out of the joints during the fatigue tests was modelled using FEA in order to explore the correlation between water concentration at the site of crack initiation and the fatigue threshold. The diffusion coefficients used in the models were those given in Table 1. The desorption in the adhesive was assumed to be the same as the absorption at 90°C. This is correct for Fickian behaviour in which the rate of transport is independent of concentration. As we are assuming Fickian diffusion in our current modelling and as the absorption plots for the adhesive at 90°C appear reasonably Fickian, this is a reasonable assumption in this instance. It is recognised, however, that there is scope for development of the analyses demonstrated in the current work to take into account concentration-dependent diffusion and anomalous moisture sorption. The joints were modelled with the tapered fillets described in Section 5.

Figure 22 shows water concentration in the adhesive at the embedded corner of the lap adherend as a function of fatigue cycles for the samples with unidirectional CFRP adherends. It is shown that in both cases that there is a large change in the moisture concentration at this point over the course of the fatigue testing.

It was considered that the maximum water concentration might provide a correlation with fatigue threshold. It can be seen in Table 2 that both the sample conditioned "wet" and tested "wet" and the sample conditioned "wet" and tested "dry" have the same fatigue threshold and will also have approximately the same maximum moisture concentration, for both UD and MD adherends. This is explored further in Figure 23, which shows a plot of a normalised fatigue threshold against maximum water concentration at the point of crack initiation.

Although limited data are available, it can be seen that there is a roughly linear variation between the maximum water concentration and the fatigue threshold. This is consistent with previous work, which has shown a linear relationship between water concentration and quasi-static strength in certain cases [28, 29]. Such a relationship provides a useful empirical tool for predicting fatigue thresholds in a sample subjected to any environmental regime in which the diffusion of moisture into the joint can be modelled.

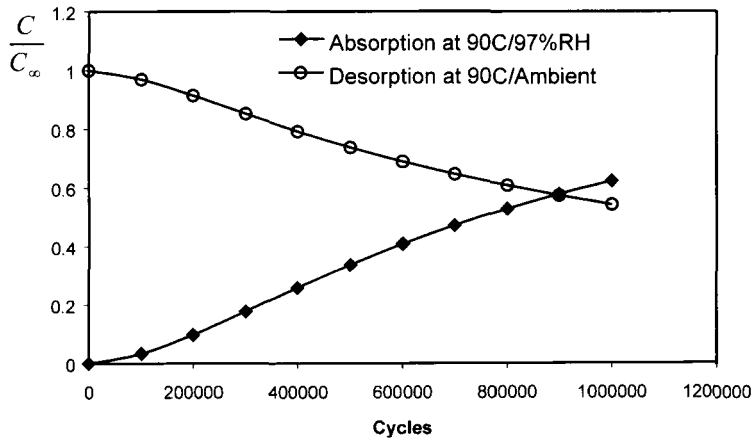

FIGURE 22 Moisture concentration *versus* fatigue cycles.

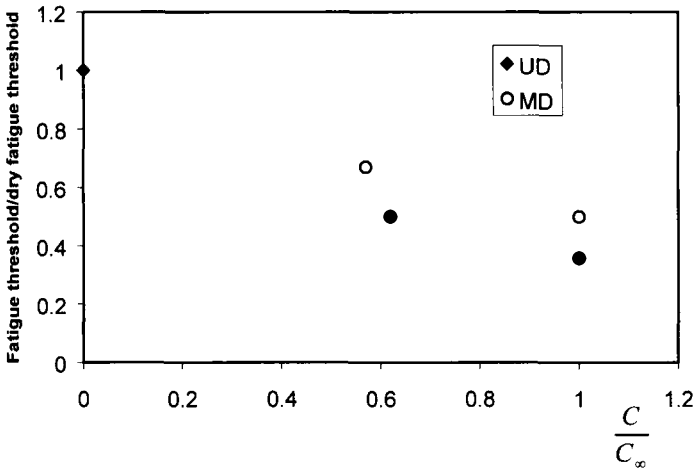

FIGURE 23 Moisture concentration *versus* fatigue cycles.

CONCLUSION

Analytical, experimental and numerical studies were presented in order to analyse the diffusion of moisture in adhesively bonded composite joints. Based on the classical theory of diffusion, equations in two-dimensional regions with prescribed boundary conditions were derived for several adhesive fillet shapes, namely radiused fillet, triangular fillet and rectangular fillet. It was found that the one-dimensional solution overestimates the retardation effect of all considered fillet types. In the experimental programme, moisture diffusion in adhesive films and in unidirectional and multidirectional composite substrates were considered in two different conditioning environments, namely 45°C/85% RH and 90°C/97% RH for the sorption studies and 90°C/ambient for the desorption studies. For the adhesive, only water sorption data were presented, while for composites both sorption and desorption data were given. Using the water uptake plots, the coefficients of diffusion were determined. For the adhesive, approximated Fickian plots were observed in both conditioning environments considered. However, for the composites Fickian behaviour was observed at 45°C/85% RH sorption and 90°C/ambient desorption, while non-Fickian behaviour was obtained at 90°C/97% RH sorption.

In contrast to the analytical solution, the finite element analysis took into consideration the moisture diffusion from the composite substrates into lap-strap joints. Unidirectional and multidirectional composites, as well as two different fillet shapes, *i.e.*, rectangular and triangular fillet, were considered in the FE analysis. From the results, it was found that when the composite becomes fully saturated, it starts to deliver a larger amount of moisture to the adhesive layer and the interface. This effect was more pronounced away from the joint edge and after a large exposed period. The comparison between the analytical and FE solution showed that the analytical solution is only applicable in case of a large ratio of fillet length to adhesive thickness. A correction factor, which can be used to fit the FEA results for different adhesive thicknesses into the analytical solution, is introduced. Finally, from fatigue test data, it was shown that there was potentially a correlation between moisture concentration and fatigue threshold, which could be used as a simple semi-empirical method of predicting the failure in joints with known moisture distributions. The analyses in this work assumed Fickian water uptake; however, the experimental data showed that in high activity environments anomalous uptake is observed. Many models to account for this anomalous behaviour have been suggested in the literature and it is proposed that in future work this aspect will be considered in more detail. However, it should also be realised that for composites and adhesives in many environments, the Fickian model is perfectly adequate. Consideration must be made, as in most engineering calculations, as to whether the gains made in increasing the accuracy of the modelling in a particular case justify the extra effort.

References

[1] Kinloch, A., *J. Adhesion* **10**, 193 (1979).
[2] Bethune, A., *SAMPE J.* **11**(14), 4 (1978).
[3] Brewis, D., Comyn, J. and Tegg, J., *Int. J. Adhes. Adhes.* **1**, 35 (1980).
[4] Glenhill, R. and Kinloch, A., *J. Adhesion*, **6**, 315 (1974).
[5] Crank, J. and Park, G., Eds., *Diffusion in polymers* (Academic Press, New York, 1968).
[6] Lefebvre, D., Dillard, D. and Ward, T., *J. Adhesion* **27**, 1 (1989).
[7] Lefebvre, D., Dillard, D. and Brinson, M., *J. Adhesion* **27**, 19 (1989).
[8] Roy, S., Lefebvre, D., Dillard, D. and Reddy, J., *J. Adhesion* **27**, 41 (1989).
[9] Kaul, A., Sung, N., Chin, I. and Sung, C., *Polym. Eng. Sci.* **24**, 493 (1984).

[10] Carslaw, H. and Jeager, J., *Conduction of heat in solids*, 2nd edition (Oxford University Press, Oxford, 1959), p. 137.
[11] Kerr, C., MacDonald, N. and Orman, S., *J. Appl. Chem.* **17**, 62 (1967).
[12] Butt, R. and Cotter, J., *J. Adhesion* **8**, 11 (1976).
[13] Brockmann, W., In: *Adhesion Aspects of Polymeric Coatings*, Mittal, K. L., Ed. (Plenum Press, New York, 1982), p. 265.
[14] *Handbook of fillers and reinforcements for plastics*, Katz, H. S. and Milewski, J. V., Eds. (Van Nostrand, New York, 1978).
[15] *Composite Materials*, Vol. 6, "Interfaces in Polymer Matrix Composites", Plueddemann, E. P., Ed. (Academic Press, New York, 1974).
[16] Crocombe, A. D., *Int. J. Adhes. Adhes.* **17**, 229 (1997).
[17] Crocombe, A. D., Hambly, H. and Pan, J., *1St World Congr. on Adhes. and Rel. Phen.*, Dechema e.V., 1.2 (1998).
[18] Ashcroft, I. A., Gilmore, R. B. and Shaw, S. J., DERA Technical Report DRA/SMC/CR961079, DRA Farnborough (1996).
[19] Ashcroft, I. A., Abdel Wahab, M. M., Crocombe, A. D., Hughes, D. J. and Shaw, S. J., *Composites Part A* **32**(1), 47-60 (2000).
[20] Abdel Wahab, M. M., Ashcroft, I. A., Crocombe, A. D., Hughes, D. J. and Shaw, S. J., *Composites Part A* **32**(1), 61-71 (2000).
[21] Crank, J., *The Mathematics of Diffusion* (Oxford University Press, Oxford, 1979).
[22] Pan, J., Crocombe, A. D., Hambly, H. O. and Megalis, P., *Presented at Adhesion 96, Institute of Materials*, Cambridge (1996).
[23] *ABAQUS Theory Manual*, Publ. Hibbit, Karlsson and Sorensen, USA.
[24] *LUSAS Theory Manual 1*, Publ. FEA Ltd., UK.
[25] Shen, C. H. and Springer, G. S., *J. Comp. Mat.* **10**, 2-20 (1976).
[26] Grayson, M. E., *J. Poly. Sci.* B **24**, 1747-1754 (1986).
[27] Bond, D., PhD Thesis, University of Surrey (1996).
[28] Brewis, D. M., Comyn, J. and Tegg, J. L., *Int. J. Adhesion and Adhesives*, **1**, 35 (1980).
[29] Brewis, D. M., Comyn, J., Cope, B. C. and Moloney, A. C., *Polymer*, **21**, 1477 (1980).